ORIGINAL ARTICLE

Interproximal periodontal defect model in dogs: a pilot study

U-W Jung, Y-Y Chang, Y-J Um, C-S Kim, K-S Cho, S-H Choi

Department of Periodontology, Research Institute for Periodontal Regeneration, College of Dentistry, Yonsei University, Seoul, Korea

OBJECTIVE: This study aimed to evaluate the validity of a surgically created interproximal periodontal defect in dogs.

MATERIALS AND METHODS: Surgery was performed in the interproximal area between the maxillary second and third premolars in two beagle dogs. Following an incision and reflection of the gingival flap, a 3-mm wide and 5-mm high defect was prepared surgically at the interproximal area. A thorough root planing was performed and the flap was coronally positioned and sutured. The contra-lateral area was served as the control with no surgical intervention. After 8 weeks of healing, the animals were killed and the defect was analysed histometrically and radiographically.

RESULTS: The interproximal periodontal defect resembled a naturally occurring defect and mimicked a clinical situation. After healing, the defect showed limited bone (0.89 ± 0.02 mm) and cementum regeneration (1.50 ± 0.48 mm).

CONCLUSIONS: Within the limitations of this pilot study, the interproximal periodontal defect showed limited bone and cementum regeneration. Thus, it can be considered as a standardized, reproducible defect model for testing new biomaterials.
Oral Diseases (2011) **17**, 26–32

Keywords: periodontal; animal models; X-ray microtomography; histology

Introduction

In order to use a new biomaterial in patients, rigorous evaluations must be conducted. Direct testing in humans would provide valuable information and the best proof-of-concept. However, human studies allow limited histological evaluation and have inherent ethical problems, although human biopsy studies have often been reported (Lee *et al*, 2008). In addition, many confounding factors, including variability in defect size, diversity of individual healing capacity, and the level of surgical skill may make it difficult to interpret the sole effect of the biomaterial. In many physiological and pathological aspects, animal models are closely similar to humans, and the use of animal models facilitates in controlling experimental conditions, like the number of subjects and healing time. Hence, numerous defect models in various animal species have been introduced as substitutes for humans in various biomaterial studies.

In general, a biomaterial is first screened through *in vitro* experiments, then evaluated *in vivo* by testing in lower order phylogenetic species, like rats and rabbits; this is followed by testing in higher order species, like dogs and nonhuman primates. In periodontal research, testing in animal models of higher order species has been preferred because of the similarity in size and morphology of the teeth. Various types of defect models with different topologies have been established, including supraalveolar (Koo *et al*, 2004; Wikesjo *et al*, 2005), dehiscence (Gineste *et al*, 2005; Graziani *et al*, 2005), furcation (Araujo and Lindhe, 1998; Araujo *et al*, 1999), 1-wall (Kim *et al*, 2002, 2005), 2-wall (Ozmeric *et al*, 2000), and 3-wall (Kim *et al*, 1998) defect models. Among these, an appropriate model can be selected according to the potential of the biomaterial.

As the number of bone wall (1-wall, 2-wall, etc) is critical in periodontal wound healing potential, the configuration of defects was classified according to the remaining number of bone walls (Goldman and Cohen, 1958) and there was a positive correlation between the number of bone walls and wound healing potential (Kim *et al*, 2004). A desirable defect model should be standardized, reproducible, and easily prepared. The supraalveolar defect model, which represents horizontal bone loss and a non-contained defect, is a well standardized model for testing the clinical potential of a biomaterial (Koo *et al*, 2004; Wikesjo *et al*, 2005). However, the supraalveolar defect model is difficult to

prepare, because the entire coronal alveolar bone around the tooth must be removed. In addition, there is a large difference between intrabony and supraalveolar defects in their degrees of difficulty in spontaneous healing. An interproximal periodontal defect (IPD), which can be categorized as a no-wall defect that faces root to root, could be ranked between these two defect models. The configuration of IPD defect in clinical situation is complicated, and is often encountered in daily practice. Nevertheless, an experimental model for an IPD has not been established.

Therefore, the purpose of this study was to evaluate the validity of a surgically created IPD in dogs.

Materials and methods

Animals
Two male beagle dogs, 15 months old and 10–15 kg, were selected. Both dogs had intact dentition and healthy periodontium. Animal selection, management, preparation, and the surgical protocol followed routine procedures that were approved by the Animal Care and Use Committee, Yonsei Medical Center, Seoul, Korea. (08-164)

Surgical procedures
The entire surgical procedure was performed under general anaesthesia that comprised a subcutaneous injection of Atropine 0.05 mg kg^{-1}, and intravenous injections of xylazine (Rompun®, Bayer Korea, Seoul, Korea) 2 mg kg^{-1} and ketamine hydrochloride (Ketalar®, Yuhan Co., Seoul, Korea) 10 mg kg^{-1} performed under sterile conditions in an operating room. The dogs were intubated, and 2% enflurane was administered. An electrocardiogram was conducted throughout the experiment. The surgical sites were disinfected and infiltration anaesthesia was performed with 2% lidocane HCl; epinephrine 1:100 000 (Kwangmyung Pharm., Seoul, Korea). A crevicular, vertical incision was made at the maxillary premolar area and the gingival flap was carefully reflected to expose the proximal bone between the second (P2) and the third premolars (P3). An IPD was surgically prepared with a fissure bur and a chisel under copious saline irrigation and thorough root planing was performed to remove the old cementum. The horizontal dimension of the defect was both 3 mm in width from the centre of the defect to the residual buccal and palatal bone, and the vertical dimension of the defect was 5 mm in height from the cemento-enamel junction (CEJ) to the apical reference notch. The reference notch was prepared at the most apical portion of the root, adjacent to the margin of the defect (Figure 1). The flaps were positioned coronally and sutured with 5-0 resorbable suture material (Polyglactin 910, braided absorbable suture, Ethicon, Johnson & Johnson Int., Edinburgh, U.K.) by the simple interrupted suture technique. The contra-lateral area between P2 and P3 was served as the control with no surgical intervention. On the day of surgery, the dogs received an intravenous injection of antibi-
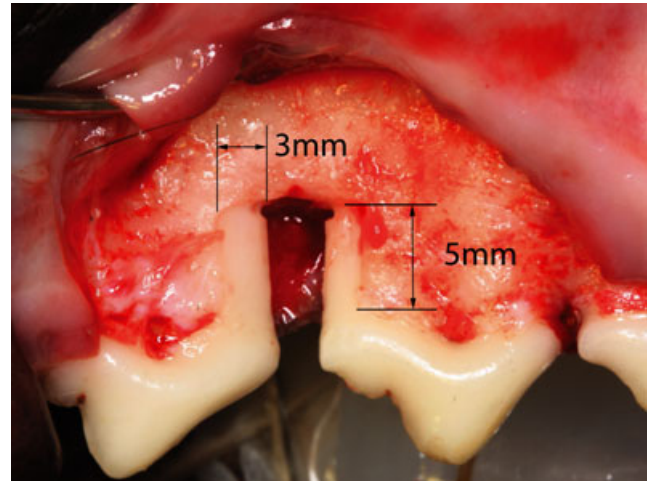
Figure 1 Clinical photograph showing the configuration of the proximal no-wall defect. The alveolar bone was removed 3 mm in width from the centre of the defect to buccal and palatal bone and 5 mm in defect height

otics at 10 mg kg^{-1} (Cefazoline Sodium 20 mg kg^{-1}, Yuhan Co., Seoul, Korea) and a topical application of a 0.2% chlorhexidine solution (Hexamedin®, Bukwang Pharmaceutical Co., Seoul, Korea), which was performed daily for infection control. Sutures were removed after 7 days and soft diet was provided throughout the study period. The dogs were killed 8 weeks after surgery. Euthanasia was performed by anaesthesia drug overdose.

Radiographic analysis: micro computed tomography (CT)
Block sections that included segments of the defects were dissected and fixed in 10% neutral buffered formalin for 10 days. The fixed block specimens were scanned in a micro-CT (SkyScan 1072®, SkyScan, Aartselaar, Belgium) at a resolution of 35 μm (100 kV, 100 μA). The scanned set of data were processed in a DICOM format and the area of interest was reconstructed with OnDemand 3D® software (Cybermed, Seoul, Korea). The overall dimensional topography of the teeth and the supporting bone was visualized with the 3-dimensionally (3-D) reconstructed image. The radiographic measurements regarding the defect height and bone regeneration (BR) were performed in the axial cross-sectional view. In the control group, the distance between the CEJ and bone crest was measured.

Histological processing
After rinsing in sterile water, the sections were decalcified in 5% formic acid, dehydrated in a graded ethanol series, and embedded in paraffin. Step-serial sections, 5-μm thick, were cut in a mesial-distal vertical plane, approximately in an 80-μm interval. The sections were stained with hematoxylin-eosin. The most central section of each defect site was selected based on the width of the root canal; this was used for the histological and histometric analyses.
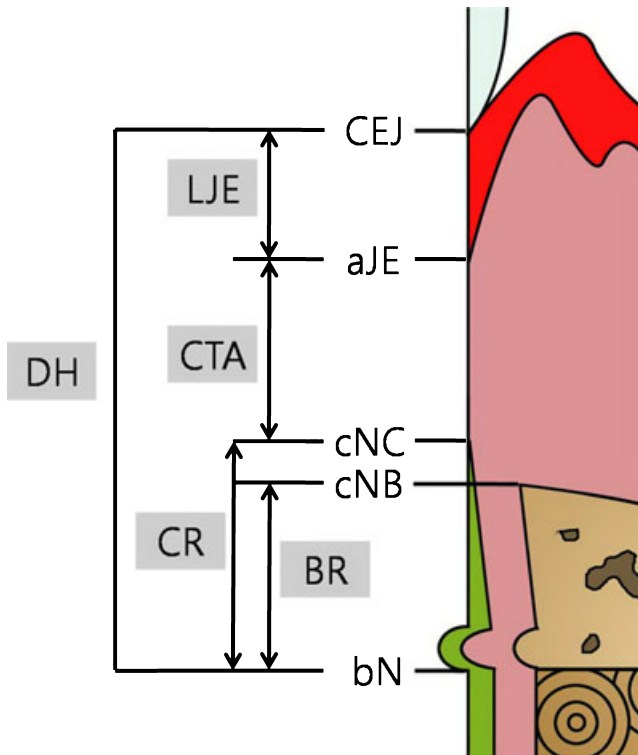
Figure 2 Schematic drawing representing measurement points for histometric analysis. CEJ, cemento-enamel junction; aJE, apical end of a junctional epithelium; cNC, coronal extension of new cementum; cNB, coronal extension of new bone; bN, base of the reference notch; DH, defect height; LJE, long junctional epithelial attachment; CTA, connective tissue attachment; CR, cementum regeneration; BR, bone regeneration

Histological and histometric analyses
Overall soft tissue healing patterns, including the degree of inflammation, bone, and attachment level were observed under a light microscope (LEICA DM-LB, LEICA, WETZLAR, Germany). An image was captured from the microscope and histometric analysis was performed with a PC-based image analysis system (Image-Pro Plus™, Media Cybernetic, Silver Spring, MD, USA). The following parameters were analysed (Figure 2):

- Defect height (DH): distance from the CEJ to the apical extension of the reference notch
- Long junctional epithelial attachment (LJE): distance from the CEJ to the apical end of a junctional epithelium
- Connective tissue attachment (CTA): distance from the end of a junctional epithelium to the coronal extension of new cementum
- Cementum regeneration (CR): distance from the apical extension of the reference notch to the coronal extension of new cementum or a cementum-like substance on the root surface
- Bone regeneration (BR): distance from the apical extension of the reference notch to the coronal extension of new bone along the root surface

In the control group, LJE and CTA were measured.

All measurements were performed on the mesial side of P3 and on the distal side of P2, and the mean value was presented.

Statistical analysis
The means and standard deviations of the measurements in the central section from each defect were analysed descriptively for both experimental and control groups.

Results

Histologic and histometric analyses
Histologic findings. The wound healing in both experimental and control groups was clinically uneventful. In the experimental group, the interproximal papilla and alveolar bone remained unfilled with collapsed tissues (Figure 3a). Inflammatory cells had infiltrated and connective tissue had degraded. The junctional epithelium had migrated apically, which resulted in the formation of a deep periodontal pocket (Figure 3b). Cementoblasts had continuously proliferated along the planed root surface, forming a cementoid (Figure 3c). Woven bone had actively formed on the crestal area. Root resorption had occurred in conjunction with the appearance of odontoclasts (Figure 3d).

In the control group, a normal dentogingival complex had formed, including intact epithelial and connective tissue attachments, and directly met the supracrestal acellular cementum (Figure 4a). Normal cementum lined the root surface up to the CEJ. The appearance of inflammatory cells around the junctional epithelium area was rare compared with the experimental group (Figure 4b). Epithelial cell rests of Malassez were observed close to the periodontal ligament (Figure 4c).

Histometric measurements. Table 1 shows the results of the histometric analysis, including measurements of DH, LJE, CTA, CR and BR. The percentage of CR and BR that corresponded to the original defect amounted to 27.17% and 16.12%, respectively (Figure 5).

Radiographic analysis: micro-CT
On the 3D reconstructed images of the experimental group, most of the root surfaces within the defect remained exposed without supporting alveolar bone (Figure 6a and b) after 8 weeks of healing (Figure 7a and b). On the axial cross-sectional images of the experimental group, interproximal BR was minimal at the centre of P2 and P3 in bucco-lingual direction (Figure 6c); in contrast, the control group clearly showed intact interproximal bone (Figure 7c). The mean BR value was 1.43 ± 0.12 mm in the experimental group, which was slightly higher than the values of histometric measurement (Table 2).

Discussion

Great innovations have been developed in the periodontal field to facilitate periodontal regeneration, including guided tissue regeneration procedures, bone grafting,
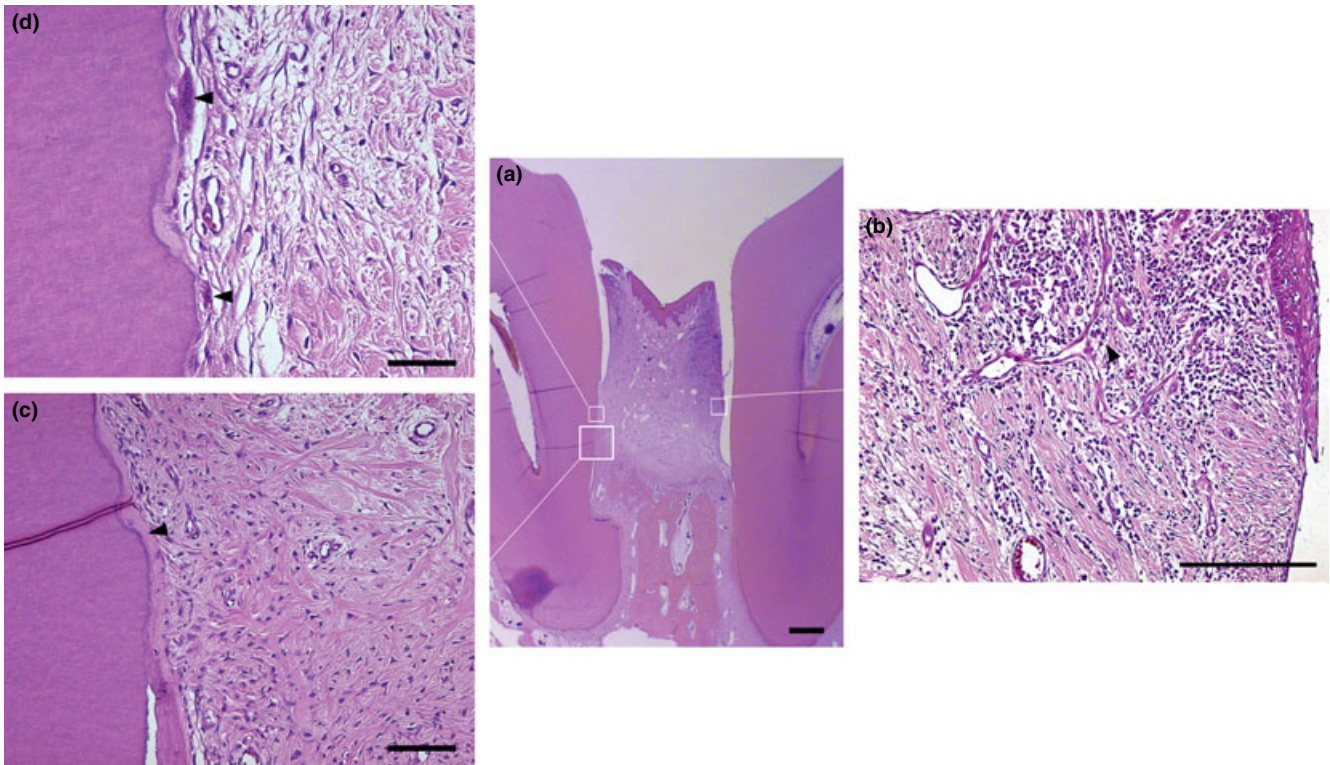
Figure 3 Histologic view of specimens from the experimental group, stained with hematoxylin-eosin. **(a)** Overall histologic view (Scale bar = 1 mm). Interproximal defect area revealed collapsed papilla and alveolar bone. Periodontal pocket was established along the root surface. **(b)** Higher magnification at the junctional epithelium (Scale bar = 0.1 mm). Infiltration of lymphocytes (arrowhead) and a large number of blood vessels were found around the periodontal pocket. **(c)** Higher magnification at the alveolar bone crest (Scale bar = 0.1 mm). Resorbed root surface was covered with cementoid (arrowhead). **(d)** Root resorption was observed at the root surface (Scale bar = 0.1 mm). Arrowhead: odontoclast
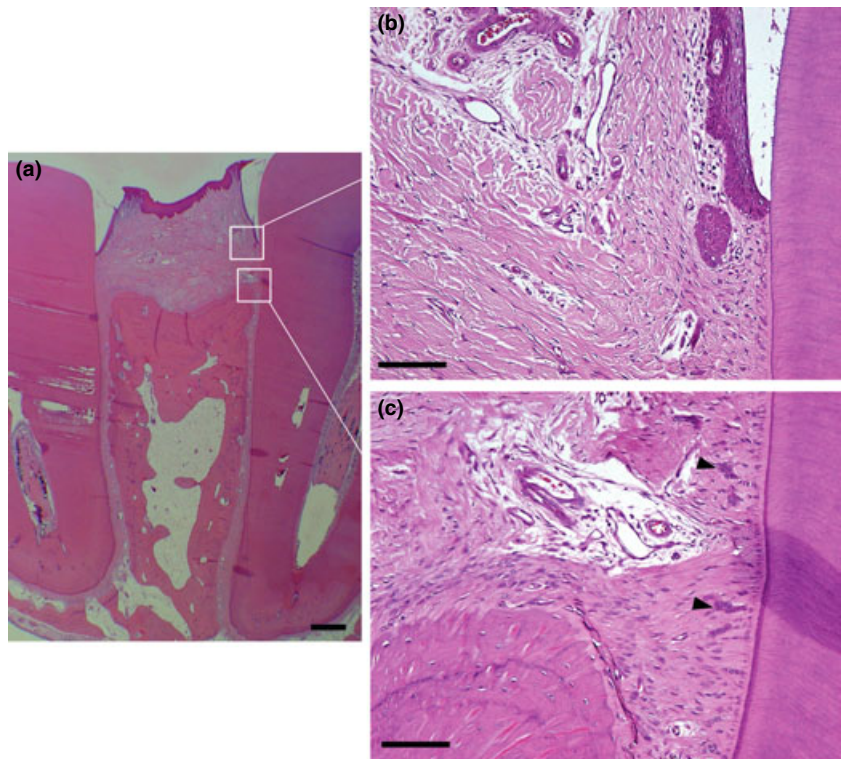
Figure 4 Histologic view of specimens from the control group, stained with hematoxylin-eosin. **(a)** Overall histologic view (Scale bar = 1 mm). Normal interproximal papilla height and alveolar bone were observed. **(b)** Higher magnification at the coronal portion (Scale bar = 0.1 mm). Intact periodontal attachment was maintained. **(c)** Insertion of the periodontal ligament fibre was perpendicular to the alveolar bone (Scale bar = 0.1 mm). Arrowhead: epithelial cell rests of Malassez

Table 1 Histometric analysis results (values represent means ± s. d.; units are mm; $N = 2$; experimental and control represent the operated and unoperated sides of the mouth, respectively)

	Experimental	Control
Defect height	5.52 ± 0.17	–
Long junctional epithelium	3.13 ± 1.08	1.58 ± 0.28
Connective tissue attachment	0.83 ± 0.50	0.80 ± 0.09
Cementum regeneration	1.50 ± 0.48	–
Bone regeneration	0.89 ± 0.02	–
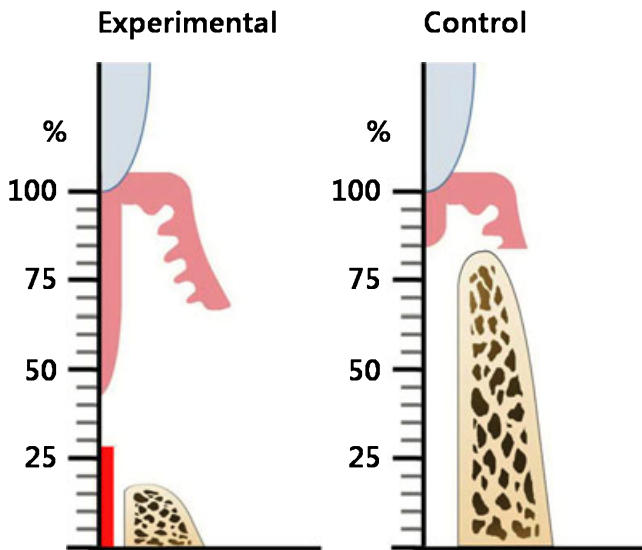
Figure 5 Histometric graph representing the measured parameters (DH, LJE, CTA, CR; red bar, and BR) in %

and tissue engineering technology. As a result of these efforts, new biomaterials have been developed. An appropriate preclinical model is critical for evaluating the safety and effectiveness of a new biomaterial prior to clinical applications. The development of tissue engineering in dental research has enhanced the regenerative potential of biomaterials; therefore, a more complicated defect is required to prove superior regenerative potential.

Experimental animals tend to present better wound healing results than humans (Sirola, 1960). Hence, the effect of a biomaterial should be tested with a consistent, standardized defect model that conforms to strict standards. This study aimed to design a 'critical sized defect', which is defined as a defect that will undergo less than 10% BR during the lifetime of the animal (Schmitz and Hollinger, 1986; Hollinger and Kleinschmidt, 1990). The defect incurred in this study did not quite achieve this goal; after 8 weeks of healing, CR and BR were 27.17% and 16.12% of the original defect size, respectively. On the contrary, the sham-surgery control of a 1-wall intrabony defect was reported to result in both CR and BR that exceeded 30% (Kim et al, 2004), and supraalveolar defects resulted in CR and BR of 27% and 18% of the defect height, respectively (Wikesjo and Nilveus, 1991). Therefore, although we failed to achieve a true critical sized defect, we did create a defect that showed more difficult spontaneous healing than that of the 1-wall defect model.

In the present study, an IPD was prepared in the maxillary premolar area of the dog. Previously, the maxillary teeth of the dog were considered unsuitable in a periodontal defect model, because of the dissimilarity of the dog and human palates, especially compared with the similarity in the mandibular teeth. Hence, most periodontal defect models were prepared at the mandibular premolar area (Kim et al, 1998, 2002, 2005; Song et al, 2005; Yeo et al, 2005). However, because dogs have four premolars and two molars in the maxilla compared with three molars in the mandible (Navia, 1977), the space between the premolars is suitable for preparing a proximal defect.

In spite of the high prevalence of IPD (Nielsen et al, 1980; Wouters et al, 1989), a standardized animal model that reproduces the clinical situation has not been
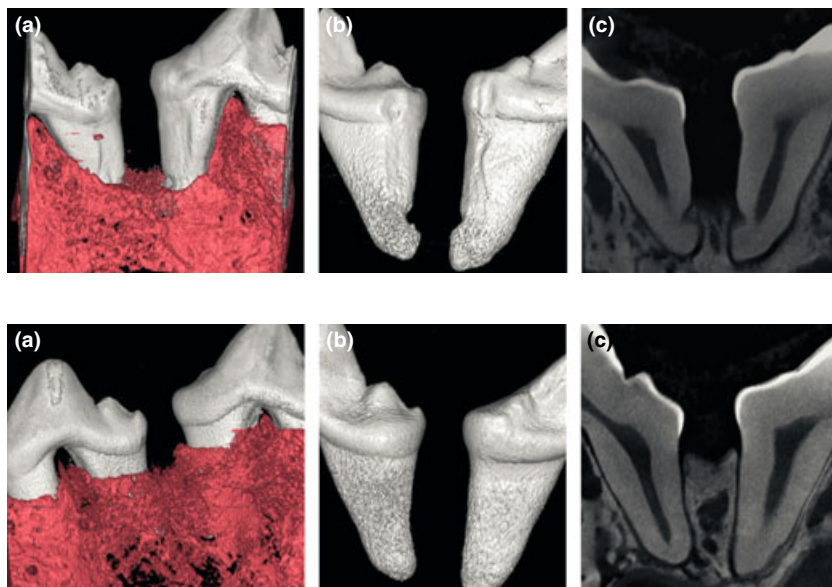
Figure 6 Radiographs of specimens from the experimental group. **(a)** The 3D image from the micro-CT. Note the limited lateral bone regeneration from the buccal and palatal bony plate. Pink area: residual alveolar bone. **(b)** The 3D reconstructed root surface. The surface of the defect area was smooth; the other areas were rather rough. **(c)** The axial cross-sectional image from the micro-CT. Interproximal bone defect remained close to the reference notch

Figure 7 Radiographs of specimens from the control group. **(a)** The 3D image from the micro-CT. Pink area: alveolar bone. **(b)** The 3D reconstructed root surface. The root surface covered with bone was rough compared with that of the experimental group. **(c)** The axial cross-sectional image of the micro-CT. The interproximal bone remained intact

Table 2 Radiographic analysis results (values represent means ± s. d.; units are mm; $N = 2$; experimental and control represent the operated and unoperated sides of the mouth, respectively)

	Experimental	Control
Defect height	5.56 ± 0.45	–
Bone regeneration	1.43 ± 0.12	–
CEJ-bone crest	4.12 ± 0.42	0.86 ± 0.07

established. The IPD model presented here could provide a standardized animal model. Moreover, this model does not require extraction of the adjacent teeth for defect preparation; thus, compared with models with intrabony defects, the experimental healing period can be reduced.

Defect configurations, including the defect depth (Selvig *et al*, 1993; Tonetti *et al*, 1993; Falk *et al*, 1997), width (Mellonig, 1984), and the angulation of the defect wall (Steffensen and Webert, 1989; Tonetti *et al*, 1993), influence the outcome of regenerative periodontal procedures. Many studies have mentioned that a defect surrounded by bony walls results in better defect filling and histologic regeneration because of better wound stability and proximity to vascular and cellular sources (Renvert *et al*, 1985; Wikesjo and Selvig, 1999; Kim *et al*, 2004). On the contrary, a non-contained defect without bony walls jeopardizes wound healing. In the IPD used in the present study, vascular and cellular sources originated from the adjacent facial and palatal bone. However, the 3D CTs in the experimental group revealed that most of the root surface within the defect remained exposed without BR from the adjacent facial and palatal bone. Hence, this factor can be excluded in the consideration of wound healing. Furthermore, the two opposing root surfaces are not vascularized and do not play a role in regeneration. Therefore, it can be assumed that the IPD could be categorized as a no-wall defect.

The surgically created acute periodontal defect was preferable to a natural plaque-induced chronic periodontal defect, because the surgical preparation of a defect can save time and allows standardization of defect size. In addition, meticulous root planing would detoxify the root surface and, consequently, would provide the same postsurgical healing to both acute and chronic defects (Isidor *et al*, 1985; Wikesjo *et al*, 1991).

Various analytic methods with radiography have been used for evaluation of regenerative therapies in clinical and experimental studies. Micro-CT allows an evaluation of the dimensional changes in 3D and the visualization of any cross-sectional slice of the specimen. These quantitative measurements of hard tissues could provide additive information in addition to the histological results. In the present study, histological findings demonstrated the formation of osteoid and cementoid tissues after an 8-week healing period. This implied that the healing process had not been completed. Future experiments should be conducted to evaluate later healing patterns in this defect and complete wound healing with a longer healing period. In addition, the proximity of the nasal cavity in the maxilla and the

interproximal distance between premolars might be different according to each animal subject. The influence of these factors should be considered in the future study.

Within the limitations of this study, the IPD showed limited bone and CR. We consider this defect model to be standardized and reproducible for testing new biomaterials.

Acknowledgements

References

Araujo MG, Lindhe J (1998). GTR treatment of degree III furcation defects following application of enamel matrix proteins. An experimental study in dogs. *J Clin Periodontol* **25:** 524–530.

Araujo MG, Berglundh T, Albrekstsson T, Lindhe J (1999). Bone formation in furcation defects. An experimental study in the dog. *J Clin Periodontol* **26:** 643–652.

Falk H, Laurell L, Ravald N, Teiwik A, Persson R (1997). Guided tissue regeneration therapy of 203 consecutively treated intrabony defects using a bioabsorbable matrix barrier. Clinical and radiographic findings. *J Periodontol* **68:** 571–581.

Gineste L, Gineste M, Bluche L *et al* (2005). Histomorphometric comparison of three bioabsorbable GTR barrier membranes in the canine model. *Int J Periodontics Restorative Dent* **25:** 61–71.

Goldman H, Cohen D (1958). The infrabony pocket: Classification and treatment. *J Periodontol* **29:** 272–291.

Graziani F, Laurell L, Tonetti M, Gottlow J, Berglundh T (2005). Periodontal wound healing following GTR therapy of dehiscence-type defects in the monkey: short-, medium- and long-term healing. *J Clin Periodontol* **32:** 905–914.

Hollinger JO, Kleinschmidt JC (1990). The critical size defect as an experimental model to test bone repair materials. *J Craniofac Surg* **1:** 60–68.

Isidor F, Karring T, Nyman S, Lindhe J (1985). New attachment-reattachment following reconstructive periodontal surgery. *J Clin Periodontol* **12:** 728–735.

Kim CK, Kim HY, Chai JK *et al* (1998). Effect of a calcium sulfate implant with calcium sulfate barrier on periodontal healing in 3-wall intrabony defects in dogs. *J Periodontol* **69:** 982–988.

Kim HY, Kim CS, Jhon GJ *et al* (2002). The effect of safflower seed extract on periodontal healing of 1-wall intrabony defects in beagle dogs. *J Periodontol* **73:** 1457–1466.

Kim CS, Choi SH, Chai JK *et al* (2004). Periodontal repair in surgically created intrabony defects in dogs: influence of the number of bone walls on healing response. *J Periodontol* **75:** 229–235.

Kim CS, Choi SH, Cho KS, Chai JK, Wikesjo UM, Kim CK (2005). Periodontal healing in one-wall intra-bony defects in dogs following implantation of autogenous bone or a coral-derived biomaterial. *J Clin Periodontol* **32:** 583–589.

Koo KT, Polimeni G, Albandar JM, Wikesjo UM (2004). Periodontal repair in dogs: analysis of histometric assessments in the supraalveolar periodontal defect model. *J Periodontol* **75:** 1688–1693.

32

Lee JH, Jung UW, Kim CS, Choi SH, Cho KS (2008). Histologic and clinical evaluation for maxillary sinus augmentation using macroporous biphasic calcium phosphate in human. *Clin Oral Implants Res* **19:** 767–771.

Mellonig JT (1984). Decalcified freeze-dried bone allograft as an implant material in human periodontal defects. *Int J Periodontics Restorative Dent* **4:** 40–55.

Navia JM (1977). *Animal models in dental research*. University of Alabama Press: Alabama, pp. 169, 170, 178.

Nielsen IM, Glavind L, Karring T (1980). Interproximal periodontal intrabony defects. Prevalence, localization and etiological factors. *J Clin Periodontol* **7:** 187–198.

Ozmeric N, Bal B, Oygur T, Balos K (2000). The effect of a collagen membrane in regenerative therapy of two-wall intrabony defects in dogs. *Periodontal Clin Investig* **22:** 22–30.

Renvert S, Garrett S, Nilveus R, Chamberlain AD, Egelberg J (1985). Healing after treatment of periodontal intraosseous defects. VI. Factors influencing the healing response. *J Clin Periodontol* **12:** 707–715.

Schmitz JP, Hollinger JO (1986). The critical size defect as an experimental model for craniomandibulofacial nonunions. *Clin Orthop Relat Res* **205:** 299–308.

Selvig KA, Kersten BG, Wikesjo UM (1993). Surgical treatment of intrabony periodontal defects using expanded polytetrafluoroethylene barrier membranes: influence of defect configuration on healing response. *J Periodontol* **64:** 730–733.

Sirola K (1960). Regeneration of defects in the calvaria. An experimental study. *Ann Med Exp Biol Fenn* **38**(Suppl 2): 1–87.

Song WS, Kim CS, Choi SH *et al* (2005). The effects of a bioabsorbable barrier membrane containing safflower seed extracts on periodontal healing of 1-wall intrabony defects in beagle dogs. *J Periodontol* **76:** 22–33.

Steffensen B, Webert HP (1989). Relationship between the radiographic periodontal defect angle and healing after treatment. *J Periodontol* **60:** 248–254.

Tonetti MS, Pini-Prato G, Cortellini P (1993). Periodontal regeneration of human intrabony defects. IV. Determinants of healing response. *J Periodontol* **64:** 934–940.

Wikesjo UM, Nilveus R (1991). Periodontal repair in dogs. Healing patterns in large circumferential periodontal defects. *J Clin Periodontol* **18:** 49–59.

Wikesjo UM, Selvig KA (1999). Periodontal wound healing and regeneration. *Periodontol* **2000**(19): 21–39.

Wikesjo UM, Selvig KA, Zimmerman G, Nilveus R (1991). Periodontal repair in dogs: healing in experimentally created chronic periodontal defects. *J Periodontol* **62:** 258–263.

Wikesjo UM, Polimeni G, Qahash M (2005). Tissue engineering with recombinant human bone morphogenetic protein-2 for alveolar augmentation and oral implant osseointegration: experimental observations and clinical perspectives. *Clin Implant Dent Relat Res* **7:** 112–119.

Wouters FR, Salonen LE, Hellden LB, Frithiof L (1989). Prevalence of interproximal periodontal intrabony defects in an adult population in Sweden. A radiographic study. *J Clin Periodontol* **16:** 144–149.

Yeo YJ, Jeon DW, Kim CS *et al* (2005). Effects of chitosan nonwoven membrane on periodontal healing of surgically created one-wall intrabony defects in beagle dogs. *J Biomed Mater Res B Appl Biomater* **72:** 86–93.